Controlling rogue waves in inhomogeneous Bose-Einstein condensates

Shally Loomba, Harleen Kaur, Rama Gupta, and C. N. Kumar*
Department of Physics, Panjab University, Chandigarh 160014, India

Thokala Soloman Raju†
Department of Physics, Karunya University, Coimbatore 641114, India
(Received 1 March 2014; published 28 May 2014)

We present the exact rogue wave solutions of the quasi-one-dimensional inhomogeneous Gross-Pitaevskii equation by using similarity transformation. Then, by employing the exact analytical solutions we have studied the controllable behavior of rogue waves in the Bose-Einstein condensates context for the experimentally relevant systems. Additionally, we have also investigated the nonlinear tunneling of rogue waves through a conventional hyperbolic barrier and periodic barrier. We have found that, for the conventional nonlinearity barrier case, rogue waves are localized in space and time and get amplified near the barrier, while for the dispersion barrier case rogue waves are localized in space and propagating in time and their amplitude is reduced at the barrier location. In the case of the periodic barrier, the interesting dynamical features of rogue waves are obtained and analyzed analytically.

DOI: 10.1103/PhysRevE.89.052915 PACS number(s): 05.45.Yv, 42.81.Dp, 52.35.Sb, 42.65.Tg

I. INTRODUCTION

Rogue waves, often described as freak waves, giant waves, abnormal waves, or monster waves, defied all attempts at their understanding until they were finally observed scientifically at the Draupner oil platform in the North sea [1]. They appear with an amplitude significantly larger than the amplitude of the surrounding wave crests [2] and disappear without the slightest trace [3]. The conditions that cause the enormous growth of rogue waves are not fully known but ongoing efforts are taking place in this regard [4,5]. They have become a subject of intense scientific research after the experimental realization of rogue waves in various nonlinear physical systems like nonlinear optical fibers [6,7], plasma [8], water wave tanks [9], etc. As a result, a vast amount of theoretical work took place to understand the dynamics of rogue waves in various fields involving nonlinear fiber optics [10–14], Bose-Einstein condensates (BECs) [15,16], atmospheric dynamics [17], plasma [18], laser-plasma interactions [19], and even econophysics [20].

In many of the above contexts, the model equations which are used to study the dynamics of rogue waves are the variants of the nonlinear Schrödinger equation (NLSE) as they can be stimulated by modulation instability which is present in NLSE [21]. It is quite fascinating to study rogue waves in BECs as the feasibility of tuning interatomic interactions through the Feshbach resonance technique [22] allows us to control the dynamics of matter rogue waves. In the context of BECs NLSE with trapping potential is also referred to as the quasi-one-dimensional (1D) Gross-Pitaevskii (GP) equation. Although it is in general difficult to obtain the exact localized solutions for the GP equation due to the nonlinear nature of the system, a great deal of attention has been paid to obtain the exact analytical solutions for the GP equation with variable coefficients due to its potential applications in BECs [23–26]. Several works are reported that involve the exact solution of the GP equation with space and/or time modulated potentials like periodic potential [27], Van der Waals potential [28], harmonic potential in one-dimensional space [29–31], and harmonic potential in three-dimensional (3D) space [32]. Being motivated by the ongoing research in this regard, it is quite interesting to obtain the rogue wave solutions for the GP equation and discuss their controllable dynamical behavior.

Here, we have employed direct ansatz and self-similarity transformation methods [33] to obtain the rogue wave solutions for the system under study. In doing so we have introduced free parameters to the system and by suitably choosing these parameters we can study the propagation of rogue waves through the systems of physical interest. In addition, we have also investigated the nonlinear tunneling of rogue waves through a conventional nonlinear and dispersion barrier and the periodic dispersion barrier.

Historically, the phenomenon of nonlinear tunneling was introduced by Newell in 1978 [34]. The investigation of nonlinear tunneling of solitons was started with the pioneering work of Serkin and Belyaeva [35]. To study the nonlinear tunneling effects for solitons they have made use of the variable-coefficient NLSE (vc-NLSE). Subsequently, nonlinear tunneling effects, governed by vc-NLSE, have been meticulously investigated. Yang *et al.* described the pulse compression through a nonlinear barrier [36]. The tunneling effects of spatial similaritons have been discussed in [37]. Dai *et al.* studied the nonlinear tunneling of bright and dark similaritons as they propagate in a birefringent fiber [38]. These days there is a renewed interest to study the nonlinear tunneling of rogue waves. In [39] nonlinear tunneling of self-similar rogue waves has been investigated and it has been revealed that the rogue waves can travel with increasing, unchanged, or decreasing amplitude depending on the ratio of the amplitude of the rogue waves and the barrier height. The tunneling effects of optical rogue waves in the femtosecond regime has also been discussed through the dispersion barrier with exponential background [40]. Zhu discussed the nonlinear

*cnkumar@pu.ac.in
†soloman@karunya.edu

tunneling of rogue waves in a graded-index waveguide [41]. To the best of our knowledge, very less attention has been paid to the study of nonlinear tunneling of rogue waves in the BEC framework.

The paper is organized as follows: In Sec. II, we present the model equation and obtain the rogue wave solutions by employing direct ansatz and similarity transformations. In Sec. III, we exemplify the controllable behavior of rogue waves. In Sec. IV, we investigate the nonlinear tunneling effect of rogue waves. Finally, concluding remarks are given in Sec. V.

II. MODEL EQUATION AND GENERAL ANALYTICAL SOLUTIONS

Here, we are focusing on the cigar shaped BEC of relatively low density, which corresponds to the case when the kinetic energy in the transverse direction is much greater than the energy of the two body interactions, i.e., $N|a_s| \ll a_\perp$ with N represents the total number of atoms, a_s is the time dependent s-wave scattering length, and $a_\perp = \sqrt{\frac{\hbar}{m\omega_\perp}}$ [24]. The evolution of the condensate is governed by the quasi-1D GP equation [24,42]

$$i\hbar\psi_t + \frac{\beta_1(t)\hbar^2}{2m}\psi_{xx} + g_1(t)|\psi|^2\psi + V(x,t)\psi = 0, \quad (1)$$

where ψ represents the macroscopic condensate density, m is the atomic mass, β_1 denotes the dispersion coefficient, g_1 is a measure of nonlinear two body interactions and is associated with the scattering length a_s which can be modulated by Feshbach resonance [22,25,43], and $V(x,t)$ is the space and time dependent potential.

Normalizing the density $|\psi|^2$, length, time, and energy in Eq. (1) in units of $2a_s$, $a_\perp = \sqrt{\frac{\hbar}{m\omega_\perp}}$, $\omega_\perp^{-1}$, and $\hbar\omega_\perp$ where $\omega_\perp$ is the transverse trapping frequency. We get the following effective 1D GP equation with time dependent dispersion $[\beta(t)]$ and nonlinearity $[g(t)]$ and time and space dependent potential $(v(x,t))$:

$$i\psi_t + \frac{\beta(t)}{2}\psi_{xx} + g(t)|\psi|^2\psi + v(x,t)\psi = 0. \quad (2)$$

This model equation has been used to describe the BECs in different experimental setups [44]. Belyaeva and Serkin have thoroughly explored this model equation to investigate the nonautonomous matter wave solitons in BECs [45]. The exact solitary wave solution of Eq. (2) (on replacing z with t) has been predicted in [46] for the case of Bessel nonlinearity. The corresponding two-dimensional GP equation has been exploited to study the 2D superfluid flows in inhomogeneous BECs [47]. By including the gain term Eq. (2) has been implemented to obtain the soliton and periodic solutions [48] and to define the snakelike traces of nonautonomous rogons [49]. Variants of Eq. (2) have been studied in the context of optical fibers as well [33,50].

Here, we are employing ansatz and similarity transformations to obtain the exact solutions for Eq. (2). After obtaining the exact rogue wave solutions we study their propagation through different systems of physical interest. Finally, we discuss the nonlinear tunneling of rogue waves through different barriers.

To begin with, substituting the ansatz

$$\psi(x,t) = [S(x,t) + iG(x,t)]\exp i\phi(x,t) \quad (3)$$

into Eq. (2) and on separating real and imaginary parts we get the set of coupled equations with variable coefficients:

$$-G_t - S\phi_t + \frac{\beta(t)}{2}\left[S_{xx} - 2\phi_x G_x - \phi_{xx}G - \phi_x^2 S\right] + g(t)(S^2+G^2)S + vS = 0, \quad (4)$$

$$S_t - G\phi_t + \frac{\beta(t)}{2}\left[G_{xx} + 2\phi_x S_x + S\phi_{xx} - {\phi_x}^2 G\right] + g(t)(S^2+G^2)G + vG = 0. \quad (5)$$

Here, functions $S(x,t)$, $G(x,t)$, and $\phi(x,t)$ are real.

Introducing new variables $\eta(x,t)$, $\chi(x,t)$, and $\tau(t)$ and employing the similarity transformation for the real functions S, G, and ϕ, we have

$$S(x,t) = M(t)[1 + nP(\eta,\tau)], \quad (6)$$

$$G(x,t) = lM(t)Q(\eta,\tau), \quad (7)$$

$$\phi(x,t) = \chi(x,t) + \mu(\tau). \quad (8)$$

Here, n and l are constants. Substituting these transformations in Eqs. (4) and (5), we deduce the following conditions:

$$\eta_{xx} = 0, \quad (9)$$

$$\eta_t + \beta\chi_x\eta_x = 0, \quad (10)$$

$$-\chi_t - \frac{{\chi_x}^2}{2}\beta + v = 0, \quad (11)$$

$$2M_t + \beta\chi_{xx}M = 0, \quad (12)$$

$$-lMQ_\tau\tau_t - M(1+nP)\mu_\tau\tau_t + n\frac{\beta}{2}{\eta_x}^2 MP_{\eta\eta} + g(t)[(1+nP)^2 + l^2Q^2]M^3(1+nP) = 0, \quad (13)$$

$$nMP_\tau\tau_t - lMQ\mu_\tau\tau_t + l\frac{\beta}{2}{\eta_x}^2 MQ_{\eta\eta} + g(t)[(1+nP)^2 + l^2Q^2]lM^3Q = 0, \quad (14)$$

where the functions $\eta(x,t)$, $\chi(x,t)$, $M(t)$, $P(\eta,\tau)$, and $Q(\eta,\tau)$ need to be determined. Solving Eqs. (9)–(12) we obtain

$$\eta = k_1(t)x + k_2(t), \quad (15)$$

$$\chi = -\frac{k_{1t}}{2\beta k_1}x^2 - \frac{k_{2t}}{\beta k_1}x + \chi_0(t), \quad (16)$$

$$v = \chi_t + \frac{{\chi_x}^2}{2}\beta, \quad (17)$$

$$M(t) = k_{10}\sqrt{k_1}, \quad (18)$$

where k_{10} is a constant, $k_1(t)$ can be associated with the inverse of pulse width, $k_2(t)$ represents the position of its center of mass, and $\chi_0(t)$ is a free function of t.

Equation (17) in the explicit form can be written as

$$v = v_2(t)x^2 + v_1(t)x + v_0(t), \tag{19}$$

where v_2, v_1, and v_0 are real functions of time and are given as

$$\begin{aligned} v_2 &= -\frac{k_{1tt}}{2\beta k_1} + \frac{k_{1t}^2}{\beta k_1^2} + \frac{k_{1t}\beta_t}{2\beta^2 k_1}, \\ v_1 &= -\frac{k_{2tt}}{\beta k_1} + 2\frac{k_{2t}k_{1t}}{\beta k_1^2} + \frac{k_{2t}\beta_t}{\beta^2 k_1}, \quad v_0 = \frac{k_{2t}^2}{2\beta k_1^2}. \end{aligned} \tag{20}$$

Equations (13) and (14) reduce to a set of constant coefficient coupled partial differential equations, which are given as

$$nP_\tau - lQ\mu_0 + lQ_{\eta\eta} + GlQ[l^2Q^2 + (1+nP)^2] = 0, \tag{21}$$

$$\begin{aligned} &-lQ_\tau + nP_{\eta\eta} - (1+nP)\mu_0 + G(1+nP)[l^2Q^2 \\ &\quad + (1+nP)^2] = 0, \end{aligned} \tag{22}$$

under the following constraints on $\tau(t)$, $g(t)$, and μ:

$$\tau(t) = \int \frac{\beta}{2}k_1^2 dt, \quad g(t) = \frac{g_0 k_1 \beta}{2{k_{10}}^2}, \tag{23}$$

$$\mu = \mu_0 \int \frac{\beta}{2}k_1^2 dt, \tag{24}$$

where μ_0 and g_0 are constants.

Following the approach given in [28,29] we obtain the simultaneous rational solution of Eqs. (21) and (22) for $g_0 = 1$ and $\mu_0 = 1$:

$$\begin{aligned} P(\eta,\tau) &= -\frac{4}{n(1+2\eta^2+4\tau^2)}, \\ Q(\eta,\tau) &= -\frac{8\tau}{l(1+2\eta^2+4\tau^2)}. \end{aligned} \tag{25}$$

Using Eq. (25) in Eqs. (6)–(8) the exact rogue wave solution of Eq. (2), following Eq. (3), can be given as

$$\psi_1 = k_{10}\sqrt{k_1}\left[1 - \frac{4+8i\tau}{1+2\eta^2+4\tau^2}\right]\exp[i(\chi+\mu)], \tag{26}$$

where η, χ, τ, and μ are given by Eqs. (15), (16), (23), and (24), respectively. In particular, for $k_1 = 1$, $\beta = g = 1$, and $k_2 = \chi_0 = 0$, Eq. (2) reduces to the standard NLSE and the matter rogue wave solution reduces to the known rogue wave solution as given in [51].

III. EXAMPLES

The dynamics of rogue waves can be controlled by suitably managing the parameters k_1 and k_2, and we are explaining it by considering the following two cases.

A. Case 1

To study the propagation of rogue waves on a constant background we are choosing $k_1 = 1.1$, $k_2 = \sin^2 t$, and $\beta = 3\cos t$. The periodic choice of dispersion parameter β results in periodic nonlinearity g and is given as

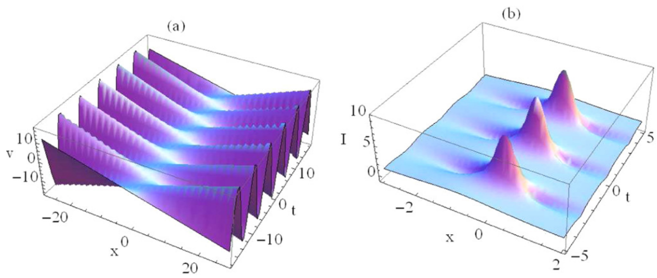

FIG. 1. (Color online) (a) Profile of potential for Eq. (28). (b) Intensity profile of rogue wave for the parameters $\beta = 3\cos t$, $k_1 = 1.1$, $k_2 = \sin^2 t$, $\mu_0 = k_{10} = 1$, $\chi_0 = 0$.

$$g(t) = 3\frac{g_0 k_1 \cos t}{2k_{10}^2}. \tag{27}$$

The corresponding potential can be worked out by using Eq. (17):

$$v(x,t) = -\frac{2x\cos t}{3k_1} + \frac{2\cos t \sin^2 t}{3k_1}. \tag{28}$$

The profile of potential is shown in Fig. 1(a), which reveals the quasiperiodic nature of the potential. Figure 1(b) shows that the rogue waves evolve periodically, in the presence of the linear (in space) potential whose amplitude is sinusoidally modulated in time. Clearly, rogue waves reoccur periodically and propagate without changing their width. The recurrence of rogue waves is due to the periodic functional form of the parameters g,β, and k_2. The rogue wave maintains the constant width and amplitude during propagation because of the absence of atomic feeding from the thermal cloud. It is evident that the nonlinearity $g(t)$ is periodic in nature, and this variation can be achieved experimentally by using a periodic magnetic or optical field near Feshbach resonance [52,53]. To be specific, nonlinearity can be positive or negative corresponding to attractive interactions (as in Li^7 [54] and Rb^{85} [55] in the BECs) or repulsive interactions (as in Rb^{87} and Na^{23} in the BECs) [23,24,56] between the atoms. As mentioned, the potential is modulated with space and time and such a potential was realized by a gravitational one [57] in earlier BEC experiments. Recently, laser beams have been used to implement linear potentials which are modulated periodically in time [58]. Moreover, in theoretical studies on nonautonomous BECs, a linear potential with an arbitrary time dependence has been reported in [59].

B. Case 2

To study the propagation of rogue waves on a periodic background we are choosing k_1 to be periodic and both the parameters k_2 and β as constants. For $k_1 = 1.1 + \cos t$, $k_2 = \beta = 1$. The nonlinearity parameter $g(t)$ and potential v read

$$g(t) = \frac{g_0(1.1+\cos t)}{2k_{10}^2}, \tag{29}$$

$$v(x,t) = v_2(t)x^2, \tag{30}$$

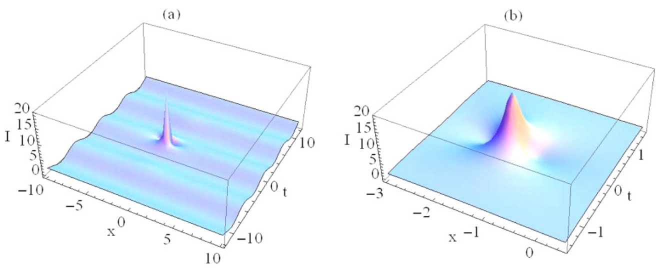

FIG. 2. (Color online) Intensity profile of rogue waves with a periodic background. (a) Periodic background and rogue wave. (b) Detailed local profile of rogue wave. The other parameters are $k_1 = 1.1 + \cos t$, $k_2 = 1$, $\beta = 1$ $\mu_0 = k_{10} = 1$, $\chi_0 = 0$.

with

$$v_2(t) = \frac{0.5(1.1\cos t + \cos^2 t + 2\sin^2 t)}{(1.1 + \cos t)^2}.$$

For the chosen parameters the intensity profile of the rogue wave is plotted in Fig. 2. Here, like the previous case the nonlinearity parameter $g(t)$ is periodic in nature and possesses only the positive value which leads to the attractive interactions as in the Li^7 or Rb^{85} case. The potential given by Eq. (30) is also time periodic and can either be confining ($v_2 < 0$) or expulsive ($v_2 > 0$). This kind of expulsive potential has been used in the experiment of [22]. Moreover, Yan *et al.* have reported such potentials in the BEC context [60] and in the optical fiber context [61].

From Figs. 1 and 2 we infer that by managing the parameters k_1 and k_2 we can control the dynamics of rogue waves. It must be noticed that the parameters k_1 and k_2 have to be chosen in such a way that the potential is well defined. For a constant dispersion parameter the desired form of nonlinearity can be obtained just by setting the value of k_1. Thus, by changing k_1 or indirectly $g(t)$ we can change the binary interactions and can study the dynamics of rogue waves for various choices of $g(t)$ through k_1. In the next section we investigate the nonlinear tunneling of rogue waves through different barriers.

IV. NONLINEAR TUNNELING OF ROGUE WAVES

To investigate the nonlinear tunneling of rogue waves, we are considering their propagation behavior for the two cases: (i) through hyperbolic nonlinearity and the dispersion barrier and (ii) through the periodic dispersion barrier.

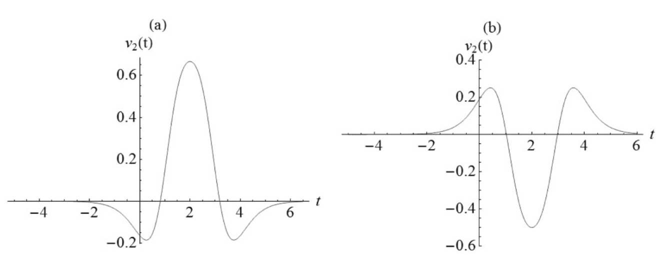

FIG. 3. Profile of quadratic potential for the (a) nonlinearity barrier case and (b) dispersion barrier case. The barrier is located at $t_0 = 2$ and the other parameters are depicted in the text for the two cases.

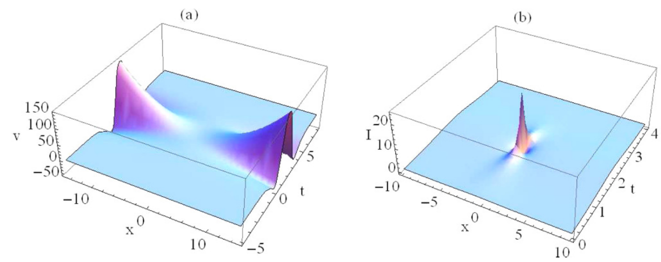

FIG. 4. (Color online) Profiles of the (a) potential given by Eq. (32) and (b) rogue wave intensity for $\beta = 1$, $k_2 = 1$, $\mu_0 = k_{10} = 1$, $\chi_0 = 0$, $h = t_0 = 2$, $\epsilon = 1$.

A. Case 1: Rogue waves tunneling through hyperbolic nonlinearity and the dispersion barrier

Here, we have chosen $k_1 = 1 + h\,\mathrm{sech}^2[\epsilon(t - t_0)]$, $\beta = k_2 = 1$. These choices lead to the following form of nonlinearity:

$$g(t) = g_0\{1 + h\,\mathrm{sech}^2[\epsilon(t - t_0)]\}, \tag{31}$$

where $g_0 = \frac{1}{2k_{10}^2}$. This represents the case of nonlinear tunneling through the nonlinearity barrier where h is the height ($h > 0$), ϵ is the barrier width, and t_0 is the location of the barrier [37]. For these parametric choices the form of the potential comes out to be

$$v(x,t) = v_2(t)x^2, \tag{32}$$

where $v_2 = \frac{p_2}{\{0.5 + h + 0.5\cosh^2[2\epsilon(t - t_0)]\}}$ with $p_2 = \epsilon^2 h\{0.75 + (0.5 + h)\cosh[2\epsilon(t - t_0)] - 0.25\cosh[4\epsilon(t - t_0)]\}\mathrm{sech}^2[\epsilon(t - t_0)]$. It is clear that Eq. (32) consists of the quadratic external potential term, which modulates its magnitude as well as its sign and changes its nature with time from attractive to repulsive to attractive [Fig. 3(a)].

The 3D profile of the potential and the intensity of rogue waves are plotted in Fig. 4 with the nonlinearity barrier located at $t_0 = 2$. For these specific choices of parameters the linear potential term is absent and the rogue waves are localized in space and time. To study the role of the nonlinearity barrier on rogue waves we have plotted the sectional plots in Fig. 5. Figure 5(a) shows that the presence of the barrier causes an increase in the amplitude of the rogue wave, and Fig. 5(b) shows that the amplification takes place only at the barrier location. This happens because the condensate is subjected

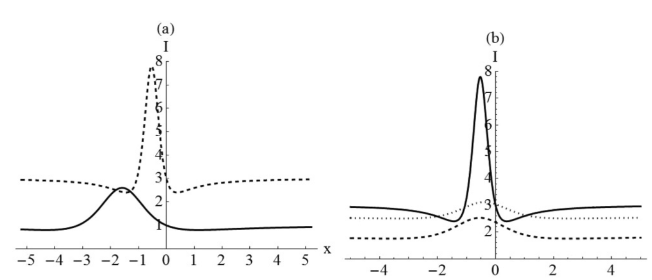

FIG. 5. Sectional plots of intensity profiles. (a) Rogue wave at $t = 2$. The solid line represents the case when the barrier is absent, and the dashed line represents the case for the barrier. (b) Intensity of rogue waves before crossing the barrier (dashed at $t = 1$), at the barrier (solid at $t = 2$), and after crossing the barrier (dotted at $t = 2.5$).

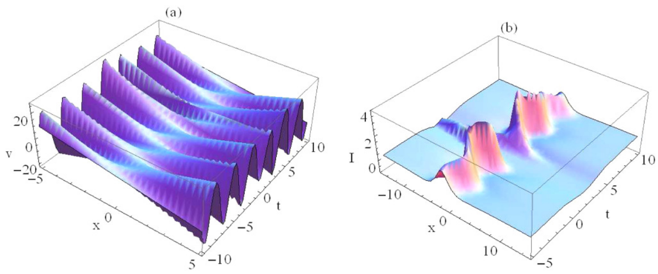

FIG. 6. (Color online) (a) Profile of potential. (b) Intensity plot for the rogue wave. The parameters are depicted in the text.

to external forcing which is varying in time and shows the maximum amplitude at the barrier location [Fig. 3(a)]. Thus, the external forcing imparts the maximum energy to the system at the barrier location. When the rogue wave is at the barrier location it exchanges the energy with the barrier and gets amplified.

To describe the effect of the dispersion barrier on nonlinear tunneling of rogue waves we are choosing [35]

$$\beta(t) = \{1 + h\text{sech}^2[\epsilon(t - t_0)]\}, \quad g(t) = g_0, \tag{33}$$

where $g_0 = \frac{1}{4k_{10}^2}$ and the other parameters are $k_2 = \sin^2 t$, $k_1 = \frac{1}{2\beta}$, $\mu_0 = k_{10} = 1$, $\chi_0 = 0$, $h = t_0 = 2$, and $\epsilon = 1$. The corresponding potential is given by Eq. (19), where the coefficients v_0, v_1, and v_2 can be obtained by substituting the values of k_1 and k_2 in Eq. (20). The explicit expressions of these can be written as $v_2(t) = \frac{4h\epsilon^2\{-3-(2+4h)\cosh[2\epsilon(t-t0)]+\cosh[4\epsilon(t-t_0)]\}}{\{1+2h+\cosh[2\epsilon(t-t_0)]\}^3}$, $v_1(t) = 2(\cos^2[t] - \sin^2[t]) + \beta\frac{4h\epsilon\sinh[2\epsilon(t-t_0)]}{\{1+2h+\cosh[2\epsilon(t-t_0)]\}^2}$, and $v_0(t) = -2\beta\cos[t]\sin[t]$.

Here, the $v_2(t)$ term represents the quadratic external potential, which is responsible for trapping the BEC. The $v_1(t)$ term contributes both the frequency shift and central position term and $v_0(t)$ contributes only to the frequency shift, which can be removed by a time dependent phase part of the wave function.

The potential profile and the intensity of rogue waves are shown in Fig. 6. Here, unlike the nonlinearity barrier case we are getting the periodic potential and propagating rogue waves; this is due to the fact that both the parameters k_1 and k_2 are time dependent and, specifically, k_2 is periodic in nature. In this case, the condensate is subjected to the quadratic potential, which is depicted in Fig. 3(b). With these modulations, the obtained rogue waves are spatially localized and propagating in time due to the parameter v_1 and the periodic nature of $v(x,t)$, which are absent in the previous case. To find the effect of the dispersion barrier on the intensity profile of rogue waves, Fig. 7 is plotted, which reveals that at the dispersion barrier the amplitude of the rogue wave is diminished and it regains its original shape after crossing the dispersion barrier. To compare with the previous case, the amplitude of the rogue wave has decreased at the dispersion barrier location, while the opposite has happened at the nonlinearity barrier location. The reason for this is that the quadratic potential term not only changes the magnitude with time but also the sign from positive to negative to positive, which means the quadratic potential is changing from repulsive to attractive and then repulsive [Fig. 3 (b)]. It should be noted that at the barrier location the v_2 amplitude is minimum (opposite to the previous case). The appearance of minimum external forcing magnitude at the barrier location causes the rogue wave to lose its energy at the barrier location. To conclude, rogue waves propagate in accordance with the parameter v_1 and when they encounter a dispersion barrier they exchange their energy with the barrier, resulting in reduction in their amplitude, and after crossing the barrier they regain their energy and start propagating as governed by v_1. It is quite interesting to control the dynamics of propagating rogue waves. We have revealed that the amplitude of the rogue waves can be decreased by making them pass through a hyperbolic dispersion barrier. Now we investigate if there is any way to increase the amplitude of the propagating rogue waves in the next case.

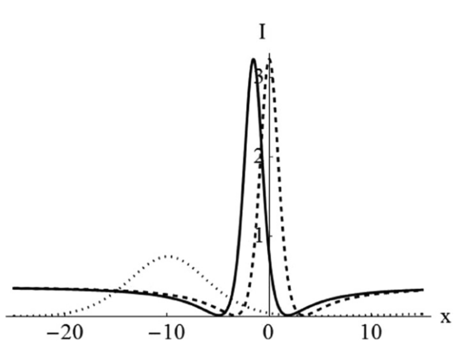

FIG. 7. Sectional plot of the intensity of rogue waves before crossing the barrier at $t = 0$ (dashed), at dispersion barrier ($t = 2$, dotted), and after crossing the barrier at $t = 4$ (line).

B. Case 2: Rogue waves tunneling through a periodic barrier

To investigate the behavior of propagating rogue waves, we are considering the parameter $k_1 = \frac{0.5}{2+h\sin^2[\epsilon(t-t_0)]}$. This choice of parameter k_1 leads to the following form of dispersion and nonlinearity parameters:

$$\beta = 2 + h\sin^2[\epsilon(t - t_0)], \quad g = g_0, \tag{34}$$

where $g_0 = \frac{0.25}{k_{10}^2}$.

This specific choice of dispersion and nonlinearity represents the case of nonlinear tunneling through a periodic dispersion barrier where h is the barrier height ($h > -2$) and ϵ is the barrier width. The corresponding potential can be worked out by using Eq. (19), and its profile is plotted in Fig. 8(a). For these choices of parameters, g, β, and k_1, the

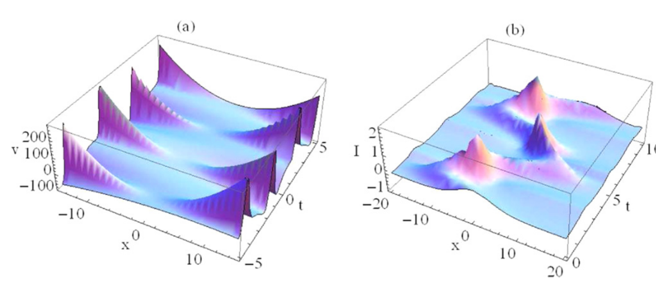

FIG. 8. (Color online) (a) Profile of periodic potential. (b) Intensity plot of rogue wave for the parameters $k_2 = \sin t$, $\mu_0 = k_{10} = 1$, $\chi_0 = 0$.

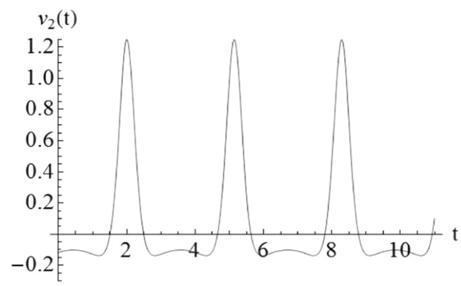

FIG. 9. The profile of quadratic potential for the parameters $k_2 = \sin t$, $\mu_0 = k_{10} = 1$, $\chi_0 = 0$.

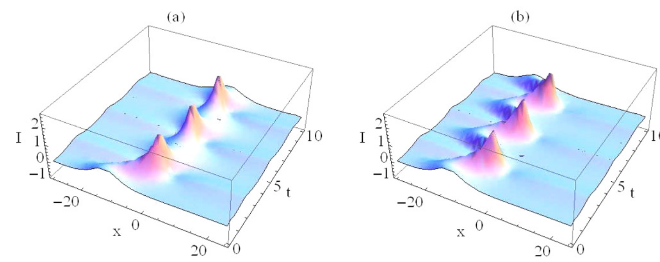

FIG. 10. (Color online) The intensity plot of rogue waves (a) for $k_2 = \text{sech}[t]$ and (b) for $k_2 = 1$ The other parameters are the same as depicted in Fig. 8.

condensate is subjected to the external quadratic potential, which is periodic in nature and gains maximum amplitude whenever it encounters the barrier location (Fig. 9). With these modulations, the system acquires maximum energy at all the barrier locations and the rogue wave exchanges the energy with the barriers and gets amplified whenever it passes through the barrier. This behavior is depicted in Fig. 8(b). As mentioned earlier, the propagation of rogue waves, in the presence of the quadratic potential, is governed by the parameter v_1, which contributes to the effect of the frequency shift and central positioning term, i.e., through k_1 and k_2. The choice of k_1 is fixed in order to get the specific dispersion barrier, while the rogue wave behavior will be different for different choices of k_2, resulting in a different functional form of v_1. To exemplify this we have plotted the profiles of rogue waves for different values of k_2 (Fig. 10) where the condensate is subjected to the same quadratic potential and the same dispersion barrier. Thus, by appropriately managing the location and the height of the barrier we can get the desired amplitude of the rogue waves at the desired location. Moreover, their propagation can be controlled by suitably choosing the parameter k_2.

V. CONCLUSION

We have presented the exact rogue wave solution for the quasi-1D GP equation, which describes the evolution of cigar shaped BECs. The solution has been obtained by using a direct ansatz and similarity transformation and is valid in general for any form of the functional parameters, provided they obey certain conditions. We have also exemplified the controllable behavior of rogue waves, with periodic nonlinearity for the two cases. For the first case BECs have been studied in the presence of the linear in space potential whose amplitude is modulated in time, while for the second case the potential is quadratic in space and can either be confining or expulsive. These potentials are experimentally realizable. In addition, we have investigated the nonlinear tunneling of rogue waves. In the case of the nonlinearity barrier, we have found that the amplitude of the localized rogue waves can be increased by arranging a barrier at their location. On the other hand, in the case of the dispersion barrier we get propagating rogue waves and their amplitude is decreased at the barrier location. The change in the amplitude of rogue waves at the barrier location is due to the exchange of their energy with the barrier and its increase or decrease is governed by the nature of the external modulations the condensate is subjected to. Interesting features are observed when the rogue waves are made to pass through the periodic dispersion barrier. Whenever the rogue waves cross the periodic barrier, their amplitude increases at the barrier location and regains its original shape after crossing the barrier. In this manner, we can get the desired amplitude of rogue waves at the desired location by adjusting the barrier height and location. Moreover, we have revealed that for a given barrier the propagation of rogue waves can be controlled by suitably choosing just the parameter k_2. The results obtained here will be useful to study rogue waves in BECs experimentally because of the space-time modulated parameters.

ACKNOWLEDGMENTS

RG would like to thank the Council of Scientific and Industrial Research, India, for financial support through Senior Research Fellowship, during the course of this work. TSR would like to thank the Department of Science and Technology, Government of India, for financial support through the Fast Track project (Young Scientist Award).

[1] W. J. Broad, *Rogue Giants at Sea* (The New York Times, 2006), http://www.nytimes.com/2006/07/11/science/11wave.html?pagewanted=all.
[2] A. R. Osborne, *Nonlinear Waves* (Academic, New York, 2009).
[3] N. Akhmediev, A. Ankiewicz, and M. Taki, Phys. Lett. A **373**, 675 (2009).
[4] P. K. Shukla, I. Kourakis, B. Eliasson, M. Marklund, and L. Stenflo, Phys. Rev. Lett. **97**, 094501 (2006).
[5] N. Akhmediev, A. Ankiewicz, and J. M. Soto-Crespo, Phys. Rev. E **80**, 026601 (2009); N. Akhmediev, J. M. Soto-Crespo, and A. Ankiewicz, Phys. Rev. A **80**, 043818 (2009).
[6] D. R. Solli, C. Ropers, P. Koonath, and B. Jalali, Nature (London) **450**, 1054 (2007).
[7] B. Kibler, J. Fatome, C. Finot, G. Millot *et al.*, Nature Phys. **6**, 790 (2010).

[8] H. Bailung, S. K. Sharma, and Y. Nakamura, Phys. Rev. Lett. **107**, 255005 (2011).

[9] A. Chabchoub, N. P. Hoffmann, and N. Akhmediev, Phys. Rev. Lett. **106**, 204502 (2011).

[10] N. Akhmediev, J. M. Dudley, D. R. Solli, and S. K. Turitsyn, J. Opt. **15**, 060201 (2013).

[11] S. Wu. Xu, J. S. He, and L. H. Wang, J. Phys. A **44**, 305203 (2011).

[12] J. S. He, S. W. Xu, and K. Porsezian, Phys. Rev. E **86**, 066603 (2012).

[13] L. J. Li, Z. W. Wu, L. H. Wang, and J. S. He, Ann. Phys. **334**, 198 (2013).

[14] J. S. He, H. R. Zhang, L. H. Wang, K. Porsezian, and A. S. Fokas, Phys. Rev. E **87**, 052914 (2013).

[15] Yu.V. Bludov, V. V. Konotop, and N. Akhmediev, Phys. Rev. A **80**, 033610 (2009); Eur. Phys. J. Special Topics **185**, 169 (2010).

[16] L. Wen, L. Li, Z. D. Li, S. W. Song, X. F. Zhang, and W. M. Liu, Eur. Phys. J. D **64**, 473 (2011); Z. Qin and G. Mu, Phys. Rev. E **86**, 036601 (2012).

[17] L. Stenflo and M. Marklund, J. Plasma Phys. **76**, 293 (2010).

[18] W. M. Moslem, Phys. Plasmas **18**, 032301 (2011).

[19] G. P. Veldes, J. Borhanian, M. Mckerr, V. Saxena, D. J. Frantzeskakis, and I. Kourakis, J. Opt. **15**, 064003 (2013).

[20] Z. Y. Tan, Commun. Theor. Phys. **54**, 947 (2010).

[21] T. B. Benjamin and J. E. Fier, J. Fluid Mech. **27**, 417 (1967).

[22] L. Khaykovich, F. Schreck, G. Ferrari, T. Bourdel, J. Cubizolles, L. D. Carr, Y. Castin, and C. Salomon, Science **296**, 1290 (2002).

[23] L. P. Pitaevskii, and S. Stringari, *Bose Einstein Condensation* (Oxford University, Oxford, 2003); F. Dalfovo, S. Giorgini, and S. Stringari, Rev. Mod. Phys. **71**, 463 (1999); O. Morsch and M. Oberthaler, *ibid.* **78**, 179 (2006).

[24] F. K. Abdullaev, A. M. Kamchatnov, V. V. Konotop, and V. A. Brazhnyi, Phys. Rev. Letts. **90**, 230402 (2003); V. A. Brazhnyi and V. V. Konotop, Mod. Phys. Lett. B **18**, 627 (2004).

[25] C. Chin *et al.*, Rev. Mod. Phys. **82**, 1225 (2010).

[26] Y. V. Kartashov, B. A. Malomed, and L. Torner, Rev. Mod. Phys. **83**, 247 (2011).

[27] J. C. Bronski, L. D. Carr, B. Deconinck, and J. N. Kutz, Phys. Rev. Lett. **86**, 1402 (2001).

[28] Yu.V. Bludov, Z. Y. Yan, and V. V. Konotop, Phys. Rev. A **81**, 063610 (2010).

[29] J. Belmonte-Beitia, V. M. Pérez-García, V. Vekslerchik, and P. J. Torres, Phys. Rev. Lett. **98**, 064102 (2007).

[30] J. Belmonte-Beitia, V. M. Pérez-García, V. Vekslerchik, and V. V. Konotop, Phys. Rev. Lett. **100**, 164102 (2008).

[31] Z. Y. Yan, X. F. Zhang, and W. M. Liu, Phys. Rev. A **84**, 023627 (2011).

[32] Z. Y. Yan and V. V. Konotop, Phys. Rev. E **80**, 036607 (2009); Z. Y. Yan and C. Hang, Phys. Rev. A **80**, 063626 (2009).

[33] S. Loomba and H. Kaur, Phys. Rev. E **88**, 062903 (2013).

[34] A. C. Newell, J. Math. Phys. **19**, 1126 (1978).

[35] V. N. Serkin and T. L. Belyaeva, JETP Lett. **74**, 573 (2001).

[36] G. Y. Yang, R. Y. Hao, L. Li., Z. H. Li, and G. S. Zhou, Opt. Commun. **260**, 282 (2006).

[37] J. F. Wang, L. Li, and S. T. Jia, J. Opt. Soc. Am. B **25**, 1254 (2008).

[38] C. Q. Dai, Y. Y. Wang, and J. F. Zhang, Opt. Express **18**, 17548 (2010); C. Q. Dai, R. P. Chen, and J. F. Zhang, Chaos, Solitons and Fractals **44**, 862 (2011).

[39] C. Q. Dai, Y. Y. Wang, Q. Tian, and J. F. Zhang, Ann. Phys. **327**, 512 (2012).

[40] C. Q. Dai, G. Q. Zhou, and J. F. Zhang, Phys. Rev. E **85**, 016603 (2012).

[41] H. P. Zhu, Nonlinear Dynamics **72**, 873 (2013).

[42] D. J. Frantzeskakis, J. Phys. A **43**, 213001 (2010).

[43] A. J. Moerdijk, B. J. Verhaar, and A. Axelsson, Phys. Rev. A **51**, 4852 (1995).

[44] J. S. He, E. G. Charalampidis, P. G. Kevrekidis, and D. J. Frantzeskakis, Phys. Lett. A **378**, 577 (2014).

[45] T. L. Belyaeva and V. N. Serkin, in *Hydrodynamics-Advanced Topics*, edited by Harry Schulz (Intech, Rijeka, Croatia, 2011), Chap. 3.

[46] W.-P. Zhong, M. R. Belic, and T. Huang, J. Opt. Soc Am. B **30**, 1276 (2013).

[47] Z. Yan, V. V. Konotop, A. V. Yulin, and W. M. Liu, Phys. Rev. E **85**, 016601 (2012).

[48] Z. Yan, Phys. Lett. A **374**, 4838 (2010).

[49] Z. Yan, Phys. Lett. A **374**, 672 (2010).

[50] S. Loomba, R. Gupta, C. N. Kumar, and D. Milovic, Appl. Mathematics and Computation **225**, 318 (2013).

[51] N. Akhmediev, J. M. Soto-Crespo, and A. Ankiewicz, Phys. Lett. A **373**, 2137 (2009).

[52] S. Inouye, M. R. Andrews, J. Stenger, H. J. Miesner, D. M. Stamper-Kurn, and W. Ketterle, Nature (London) **392**, 151 (1998); S. L. Cornish, N. R. Claussen, J. L. Roberts, E. A. Cornell, and C. E. Wieman, Phys. Rev. Lett. **85**, 1795 (2000).

[53] F. K. Fatemi, K. M. Jones, and P. D. Lett, Phys. Rev. Lett. **85**, 4462 (2000); M. Theis, G. Thalhammer, K. Winkler, M. Hellwig, G. Ruff, R. Grimm, and J. H. Denschlag, *ibid.* **93**, 123001 (2004).

[54] K. E. Strecker, G. B. Partridge, A. G. Truscott, and R. G. Hulet, Nature (London) **417**, 150 (2002).

[55] S. L. Cornish, S. T. Thompson, and C. E. Wieman, Phys. Rev. Lett. **96**, 170401 (2006).

[56] P. G. Kevrekidis, D. J. Frantzeskakis, and R. Carretero-Gonzalez, *Emergent Nonlinear Phenomena in Bose Einstein Condensates: Theory and Experiment* (Springer, New York, 2008).

[57] B. P. Anderson and M. A. Kasevich, Science **282**, 1686 (1998).

[58] H. Lignier, C. Sias, D. Ciampini, Y. Singh, A. Zenesini, O. Morsch, and E. Arimondo, Phys. Rev. Lett. **99**, 220403 (2007).

[59] Q.-Y. Li, Z.-D. Li, S.-X. Wang, W.-W. Song, and G. Fu, Opt. Commun. **282**, 1676 (2009).

[60] Z. Yan and D. Jiang, Phys. Rev. E **85**, 056608 (2012).

[61] Z. Yan and C. Dai, J. Opt. **15**, 064012 (2013).